L/Z-ligand type amphoterism of an acridinium unit

Elishua D. Litle, Shantabh Bedajna and François P. Gabbaï*

Supporting Information

Contents

1 Experimental

1.1 General experimental

All reactions and manipulations were carried out under an atmosphere of dry, O_2-free nitrogen using standard double-manifold techniques with a rotary oil pump unless otherwise stated. A nitrogen-filled glove box was used to manipulate solids, store air-sensitive starting materials, carry out room temperature reactions, recover reaction products and prepare samples for analysis. All solvents were dried by refluxing under N_2 over Na/K (Et_2O), Na (Hexanes) or CaH_2 (CH_3CN, CH_2Cl_2, $C_2H_4Cl_2$) and stored under a nitrogen atmosphere over 3Å molecular sieves. The deuterated solvents (CD_2Cl_2, $CDCl_3$, CD_3CN) used in this work were distilled over CaH_2 and were stored under a nitrogen atmosphere over 3Å molecular sieves. DMSO-d_6 was purchased from commercial suppliers and used as received. $[Rh(COD)Cl]_2$ and $[Rh(COE)_2Cl]_2$ were purchased from TCI America and used as received. ^1H, ^{13}C and $^{31}P\{^1H\}$ NMR spectra were recorded on a Bruker Avance NEO 400, a Varian VnmrS 500, or a Bruker Avance 500 cold probe spectrometer. The ^{31}P HPDec-MAS NMR experiment was carried out on a Bruker Avance-400 solid-state NMR spectrometer (400 MHz for ^1H nuclei) equipped with a standard 4-mm MAS probe head. ^1H and ^{13}C chemical shifts are expressed as parts per million (ppm, δ) downfield of tetramethylsilane (TMS) and are referenced to $CDCl_3$ (7.26/77.16 ppm), CD_3CN (1.94/1.32 ppm) or CD_2Cl_2 (5.32/53.84 ppm) as internal standards. Phosphorus (^{31}P) spectra were referenced to H_3PO_4. The NMR spectrum of [**2**][OTf] was collected at 233 K by precaution, to slow down a possible exchange of the MeCN ligands. Abbreviations used for signal description include: s for singlet, d for doublet, t for triplet, m for multiplet and br for broad. All coupling constants are absolute values and are expressed in Hertz (Hz). Elemental analyses were performed by Atlantic Microlab (Norcross, GA). The starting material [$\mathbf{L^{acr}}$]OTf was synthesized as previously described.[1]

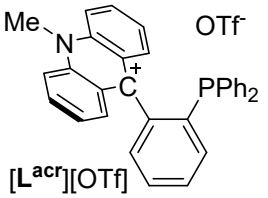

1.2 Synthesis

Synthesis of [**1**][OTf]

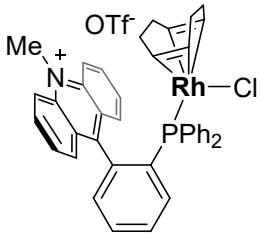

[$\mathbf{L^{acr}}$][OTf] (53.6 mg, 0.090 mmol) was dissolved in CH_2Cl_2 (1 mL) in a 20 mL scintillation vial under nitrogen. $[Rh(COD)Cl]_2$ (22.2 mg, 0.045 mmol) was added to the solution. The resulting solution was stirred for 10 minutes and treated with Et_2O (10 mL) which induced the precipitation of a red/brown solid. This precipitate was isolated by filtration and washed with Hexanes (3 x 10 mL) to afford [**1**][OTf]. Yield: 55.7 mg, 74.2%. Orange needle-like single crystals were obtained by layering Et_2O on a $C_2H_4Cl_2$ solution of [**1**][OTf]. **^{1}H NMR** (500 MHz, $CDCl_3$, 298 K) δ/ppm: 9.14 (dd, *J* = 14.8, 7.9 Hz, 1H), 8.48 (d, *J* = 9.2 Hz, 2H), 8.19 (ddd, *J* = 8.8, 6.7, 1.5 Hz, 2H), 7.97 (tt, *J* = 7.8, 1.4 Hz, 1H), 7.90 (dd, *J* = 8.6, 1.4 Hz, 2H), 7.72 (tt, *J* = 7.6, 1.5 Hz, 1H), 7.56 – 7.45 (m, 3H), 7.19 (tt, *J* = 7.5, 3.5 Hz, 2H), 7.10 – 7.04 (m, 1H), 7.03 – 6.89 (m, 4H), 6.80 (dt, *J* = 8.0, 4.0 Hz, 4H), 5.51 – 5.47 (m, 2H), 4.81 (s, 3H), 3.05 (dt, *J* = 5.9, 2.9 Hz, 2H), 2.41 – 2.22 (m, 4H), 2.06 – 2.00 (m, 2H), 1.87 (dt, *J* = 14.3, 6.8 Hz, 2H). **^{13}C NMR** (126 MHz, $CDCl_3$, 298 K) δ/ppm: 160.16, 141.42, 141.21, 140.62, 139.19, 136.04, 134.15 (d, *J* = 11.2 Hz), 132.77, 132.49, 131.23, 130.53, 130.41, 129.28, 129.16, 127.78, 127.69, 127.64, 127.56, 127.48, 126.49, 122.36, 119.81, 118.36, 105.19 – 104.91 (m), 71.36 (d, *J* = 13.3 Hz), 39.21, 33.09 (d, *J* = 2.7 Hz), 29.04. **^{31}P{^{1}H} NMR** (162 MHz, CD_2Cl_2, 298 K) δ/ppm: 33.95 (d, $^1J_{P–Rh}$ = 150.7 Hz). **Elemental Analysis** for $C_{41}H_{37}ClF_3NO_3PRhS(C_2H_4Cl_2)_{0.25}$: C: 56.97; H: 4.38 (Calc.). C: 56.67; H: 4.24 (Found).

Synthesis of [**2**][OTf]

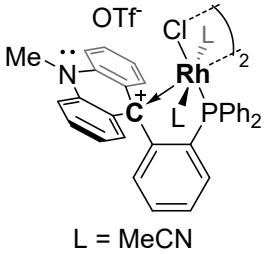

L = MeCN

[$\mathbf{L^{acr}}$][OTf] (30 mg, 0.050 mmol) was dissolved in CH_3CN (2 mL) in a 20 mL scintillation vial under nitrogen. $[Rh(COE)_2Cl]_2$ (18 mg, 0.025 mmol) was added to the solution. The resulting solution was stirred for 7 days until the solution turned to a dark red color. The solution was mixed with Et_2O (2 mL) and allowed to stir for 1 hour. This solution was then treated with an additional 5 mL of Et_2O which induced the precipitation of a dark red solid. This precipitate was isolated by decantation and washed with Et_2O (3 x 1 mL) to afford a crystalline powder of [**2**][OTf]. Yield: 36.0 mg, 88% yield. Dark red, block-like single crystals were obtained by layering Et_2O onto a CH_3CN/Et_2O solution of [**2**][OTf]-Et_2O. **^{1}H NMR** (500 MHz, CD_3CN, 298 K) δ/ppm: δ 7.92 (ddd, *J* = 11.7, 8.4, 1.4 Hz, 4H), 7.78 – 7.64 (m, 3H), 7.62 – 7.53 (m, 3H), 7.50 (tdd, *J* = 8.2, 2.9, 1.3 Hz, 4H), 7.15 (ddd, *J* = 8.5, 7.0, 1.6 Hz, 2H), 7.02 (dd, *J* = 8.4, 1.2 Hz, 2H), 6.58 (ddd, *J* = 8.1, 7.0, 1.2 Hz, 2H), 6.50 (dd, *J* = 7.9, 1.6 Hz, 2H), 3.47 (s, 3H), 2.37 (s, 6H). **^{13}C NMR** (126 MHz, CD_3CN, 298 K) δ/ppm: 161.16 (d, *J* = 25.2 Hz), 141.48, 134.01, 133.71 (d, *J* = 9.1 Hz), 133.30, 133.17, 132.22, 131.87 (d, *J* = 3.1 Hz), 128.58, 128.49, 128.16 (d, *J* = 7.6 Hz), 127.06, 126.63, 126.15, 121.87 (d, *J* = 8.2 Hz), 119.61, 112.53, 63.02 (d, *J* = 18.3 Hz), 33.88. **^{31}P{^{1}H} NMR** (162 MHz, CD_3CN, 298 K) δ/ppm: 52.95 (d, $^1J_{P-Rh}$ = 128.4 Hz). **Elemental Analysis** for $C_{36}H_{31}ClN_3PRhSO_3CF_3$: C: 53.93; H: 3.79 (Calc.).C: 53.95; H: 3.86 (Found). This analysis was carried out using crystals of [**2**][OTf]-Et_2O. The results indicate loss of the Et_2O interstitial solvent molecules during shipping and handling.

Synthesis of [**3**][OTf]

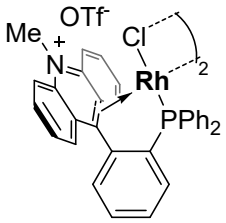

[$\mathbf{L^{acr}}$][OTf] (120 mg, 0.20 mmol) was dissolved in CH_2Cl_2 (2 mL) in a 20 mL scintillation vial under nitrogen. $[Rh(COE)_2Cl]_2$ (71.8 mg, 0.1 mmol) was added to the solution. The resulting solution was stirred for 30 minutes until the solution turned to a dark green color. The solution was treated with Hexanes (10 mL), leading to the formation of a dark green powder. This precipitate was isolated by filtration and washed with hexanes (3 x 10 mL) to afford [**3**][OTf]. Yield: 128.8 mg, 86.8%. Dark green, block-like single crystals were obtained by slow evaporation of a dichloromethane and diethyl ether solution of [**3**][OTf]. **^{1}H NMR** (500 MHz, CD_2Cl_2, 298 K) δ/ppm: 8.12 (s, 2H), 7.89 (br s, 2H), 7.69 (m, 2H), 7.63 (s, 3H), 7.49 (m 8H), 7.19 (t, *J* = 7.6 Hz, 2H), 7.09 (d, *J* = 7.9 Hz, 1H), 6.68 (d, *J* = 8.1 Hz, 2H), 3.86 (br s, 3H). **^{31}P{^{1}H} NMR** (162 MHz, CD_2Cl_2, 298 K) δ/ppm: 64.71 (d, *J* = 135.3 Hz). **Elemental Analysis** for $C_{32}H_{25}ClNPRhSO_3CF_3$: C: 53.42; H: 3.40; N: 1.89 (Calc.). C: 53.85; H: 3.70; N: 2.06 (Found).

2 NMR spectra

2.1 NMR spectra of products

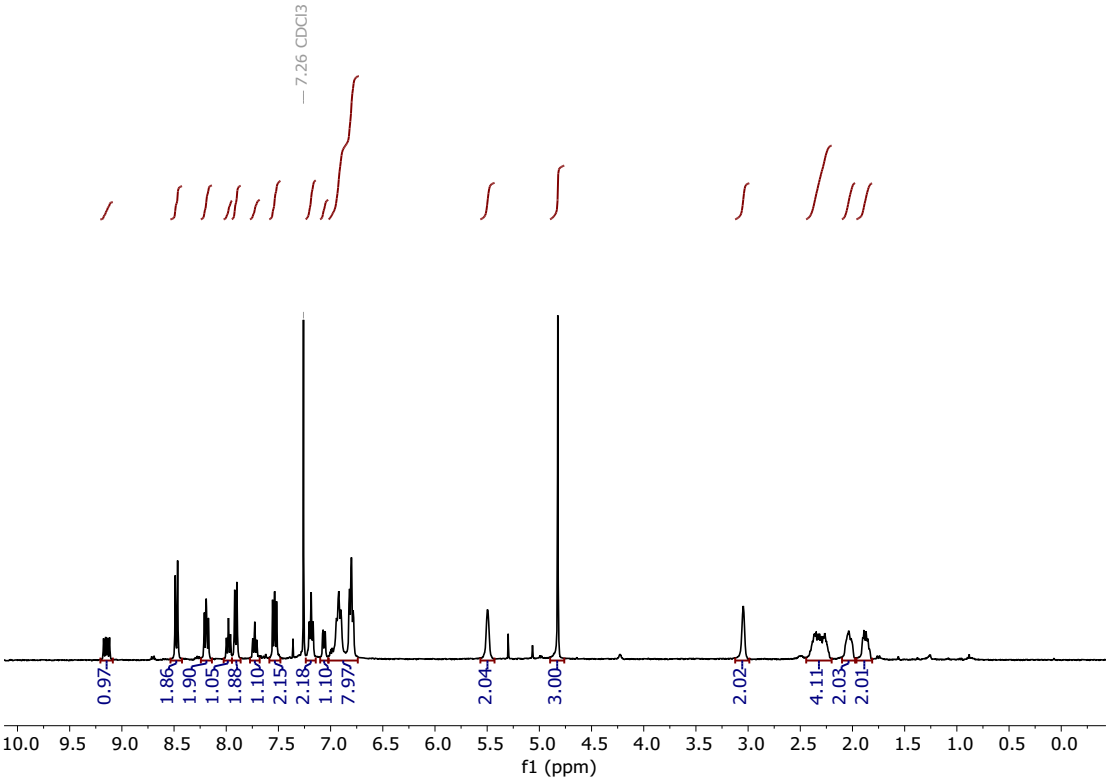

Figure S1. ^{1}H NMR (400 MHz, $CDCl_3$, 298 K) spectrum of [**1**][OTf].

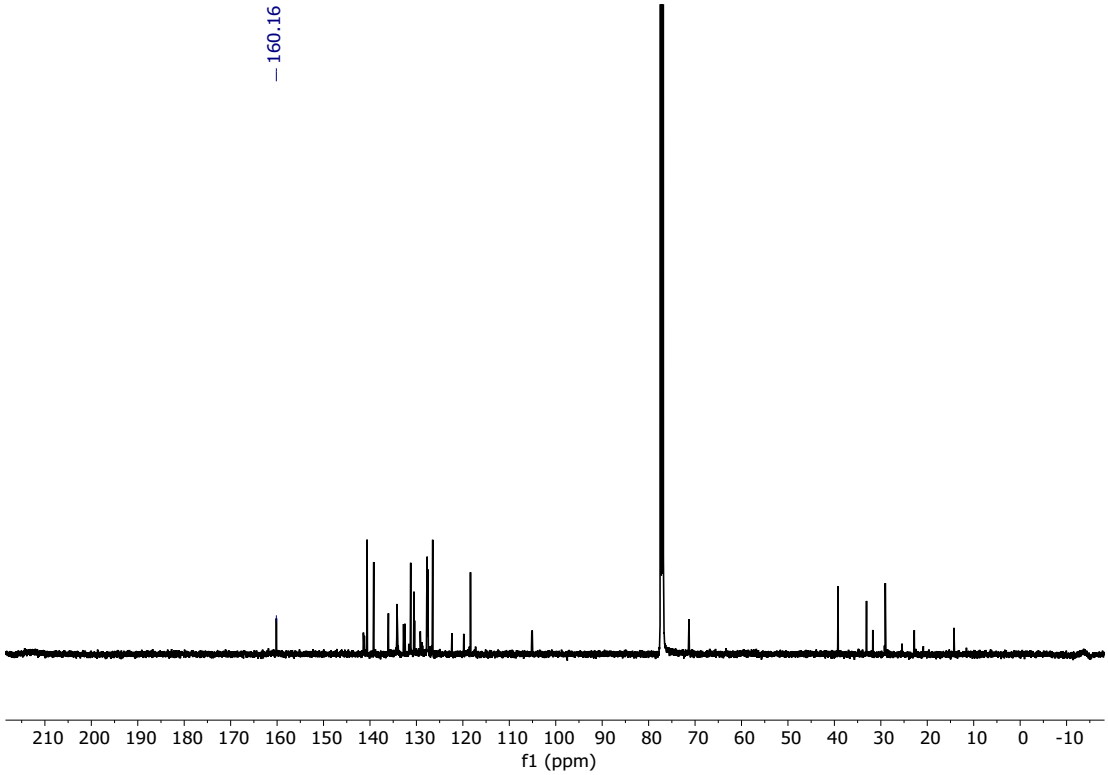

Figure S2. $^{13}C\{^{1}H\}$ NMR (126 MHz, $CDCl_3$, 298K) spectrum of [**1**][OTf].

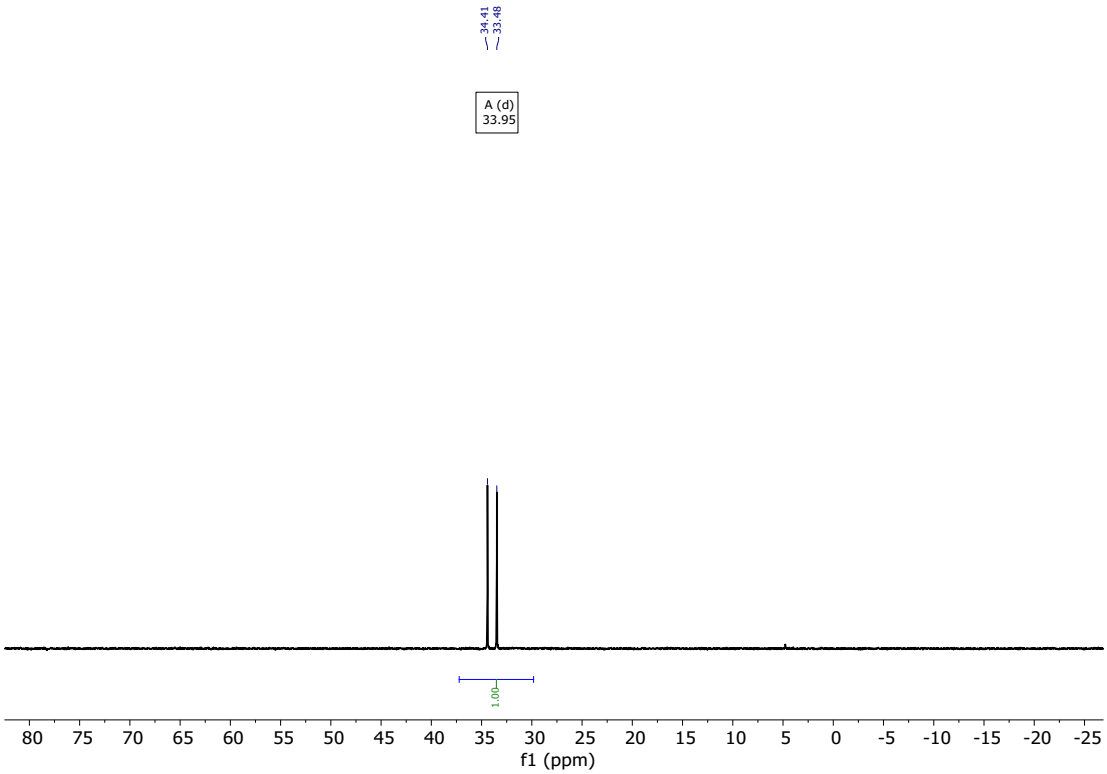

Figure S3. $^{31}P\{^{1}H\}$ NMR (202 MHz, $CDCl_3$, 298 K) spectrum of [**1**][OTf].

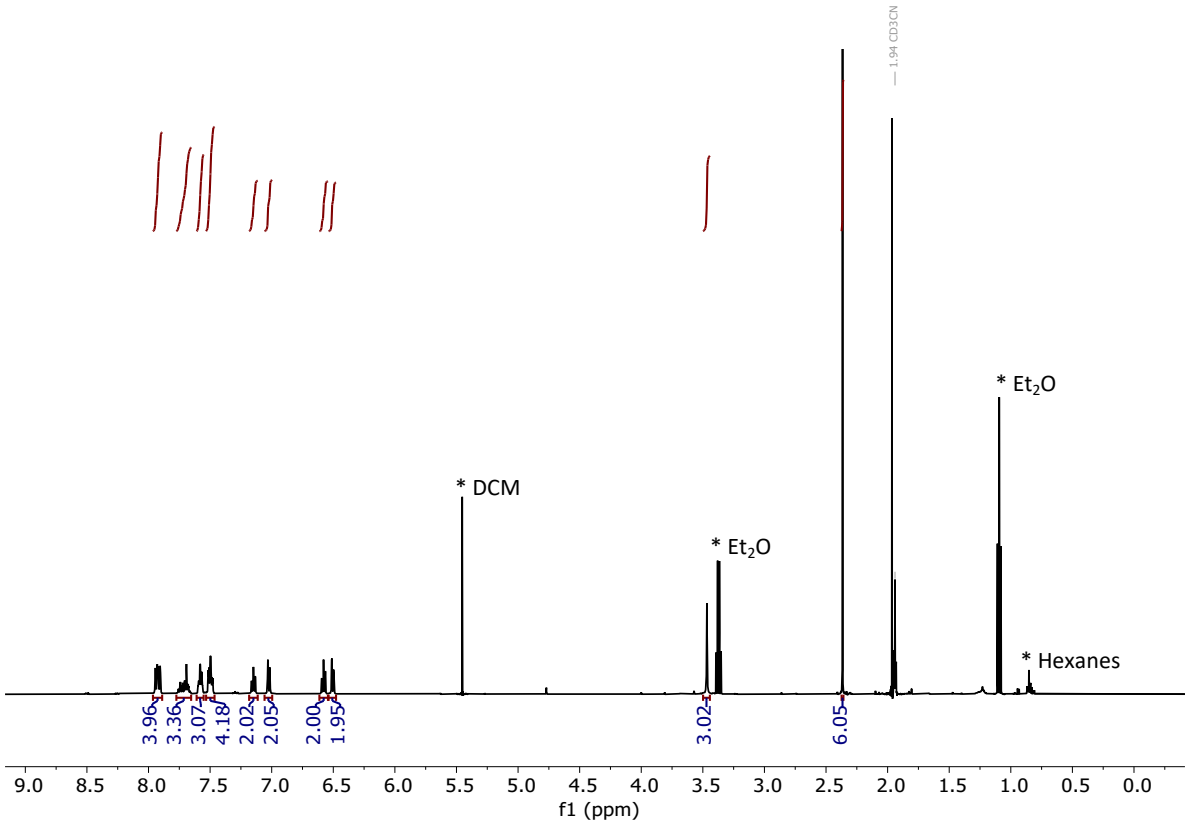

Figure S4. ^{1}H NMR (500 MHz, CD_3CN, 233 K) spectrum of [**2**][OTf].

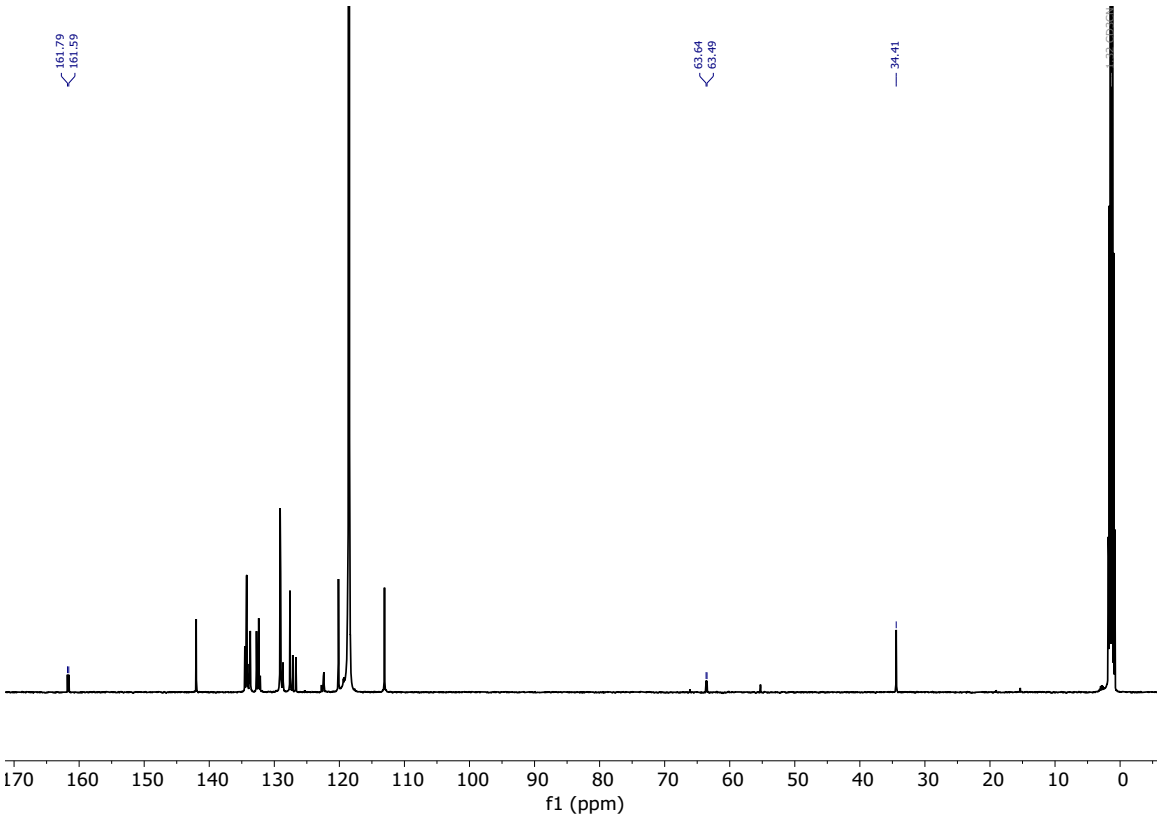

Figure S5. $^{13}C\{^{1}H\}$ NMR (126 MHz, CD_3CN, 233K) spectrum of [**2**][OTf].

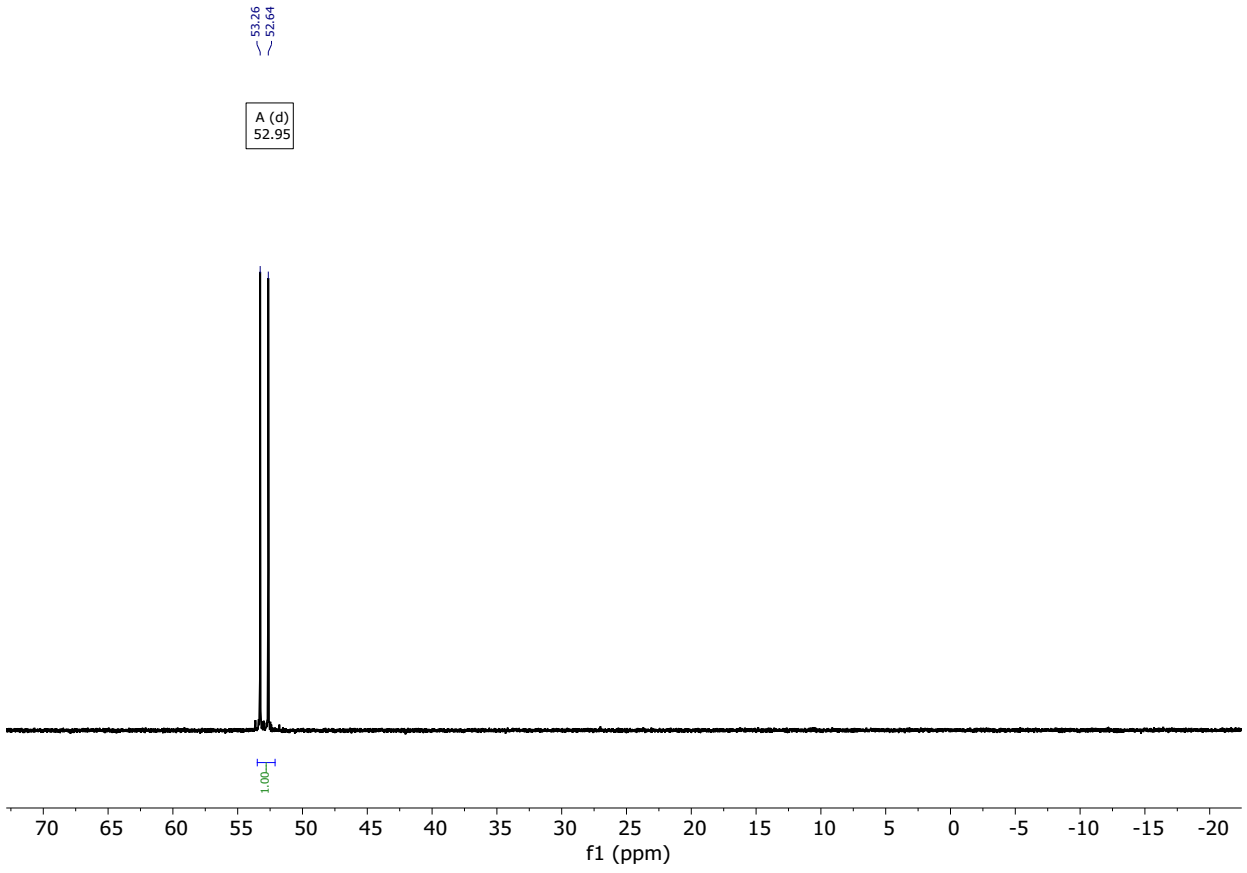

Figure S6. $^{31}P\{^{1}H\}$ NMR (202 MHz, CD_3CN, 233 K) spectrum of [**2**][OTf].

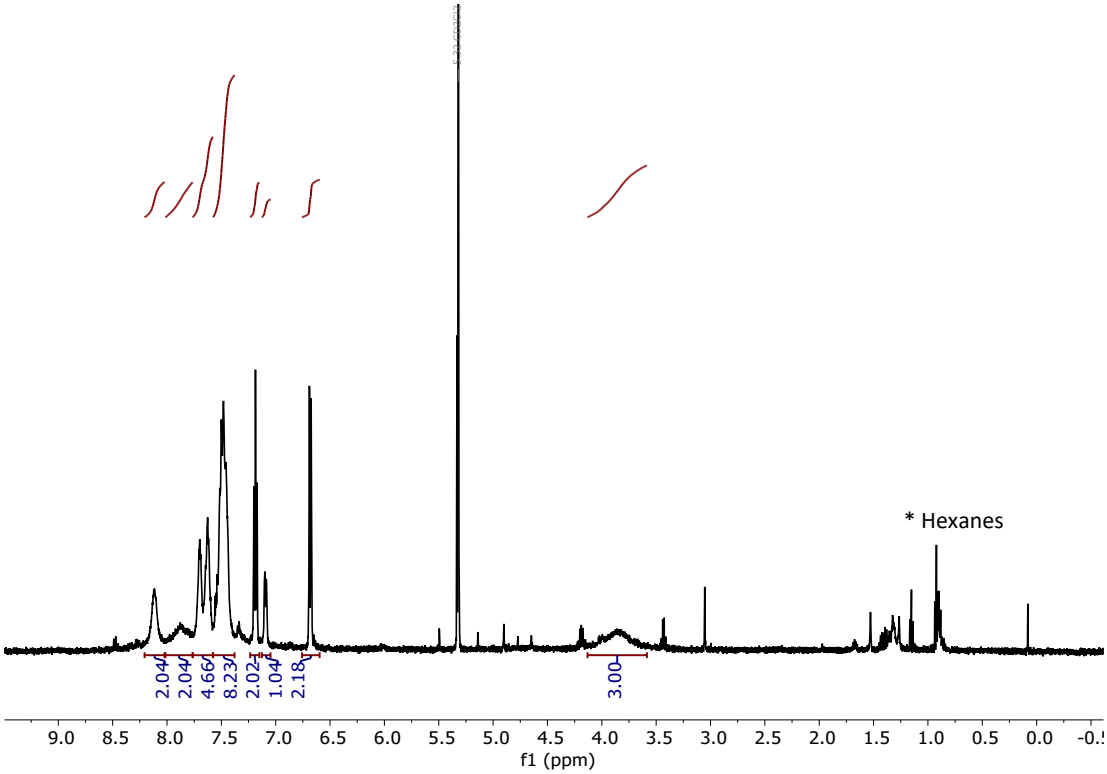

Figure S7. ^{1}H NMR (500 MHz, CD_2Cl_2, 298 K) spectrum of [**3**][OTf]. The poor quality of this spectrum reflects the low solubility of the complex.

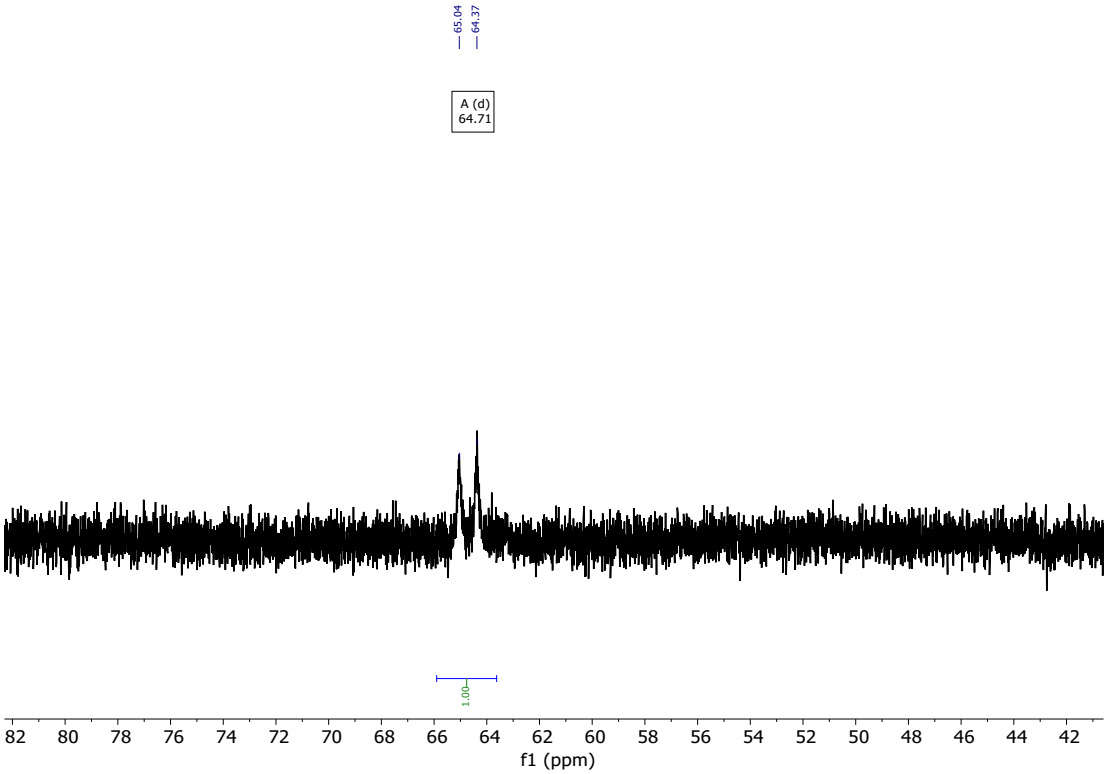

Figure S8. $^{31}P\{^{1}H\}$ NMR (162 MHz, CD_2Cl_2, 298 K) spectrum of [**3**][OTf].

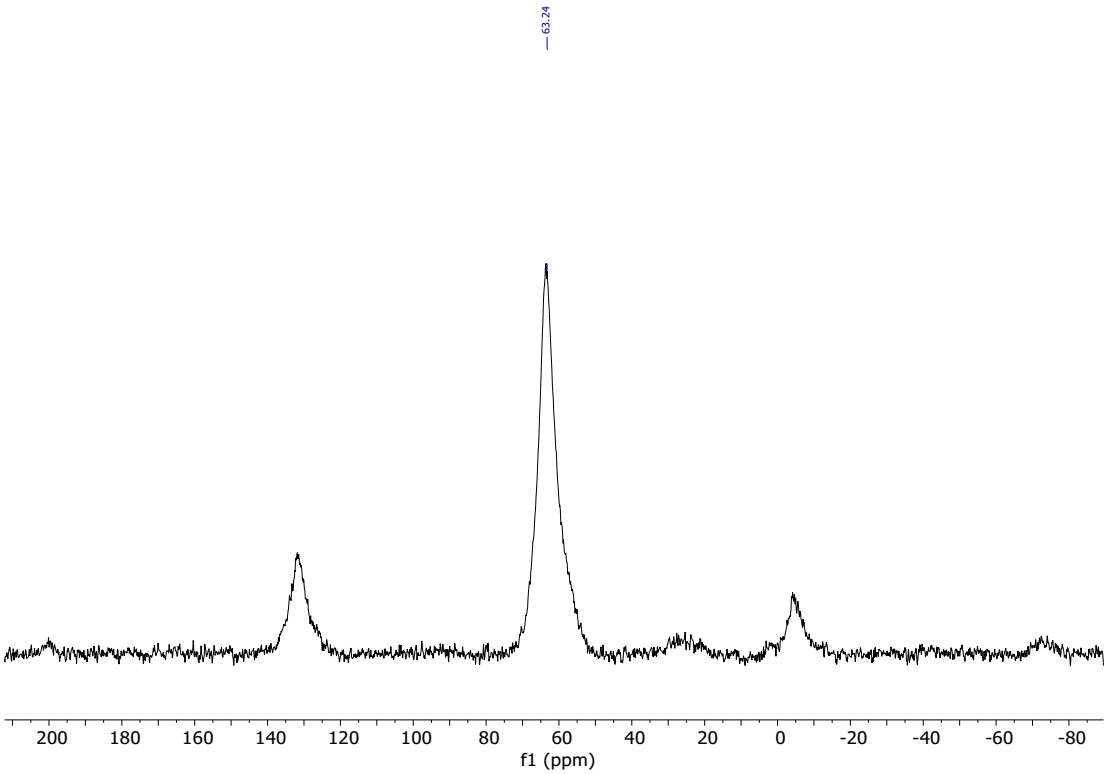

Figure S9. Solid-state ^{31}P NMR (162 MHz, 298 K) spectrum of [**3**][OTf].

2.2 NMR spectra of reactions

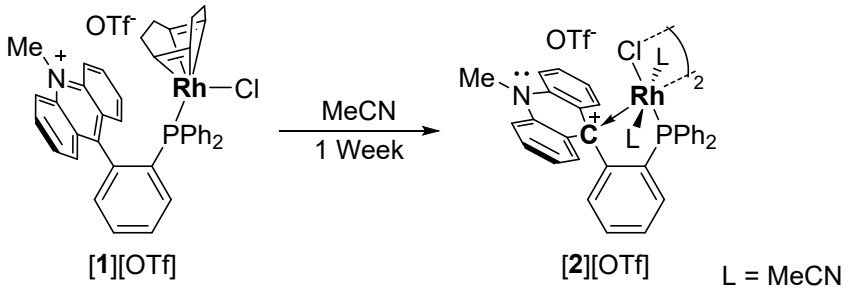

Conversion of [**1**][OTf] into [**2**][OTf]: [**1**][OTf] (10 mg), dissolved in CD_3CN (0.6 mL) was loaded into a J. Young tube and. An initial $^{31}P\{^1H\}$ NMR spectrum was collected, showing a broadening of the signal corresponding to [**1**][OTf] at 33.88 ppm. Additional spectra were collected every 24 hours over a week. The signal at 33.88 ppm gradually disappeared while that of [**2**][OTf] at 53.68 ppm gained intensity. In the course of this experiment, the solution's color changed from yellow to a dark red. Single crystals of [**2**][OTf] could be grown from this reaction.

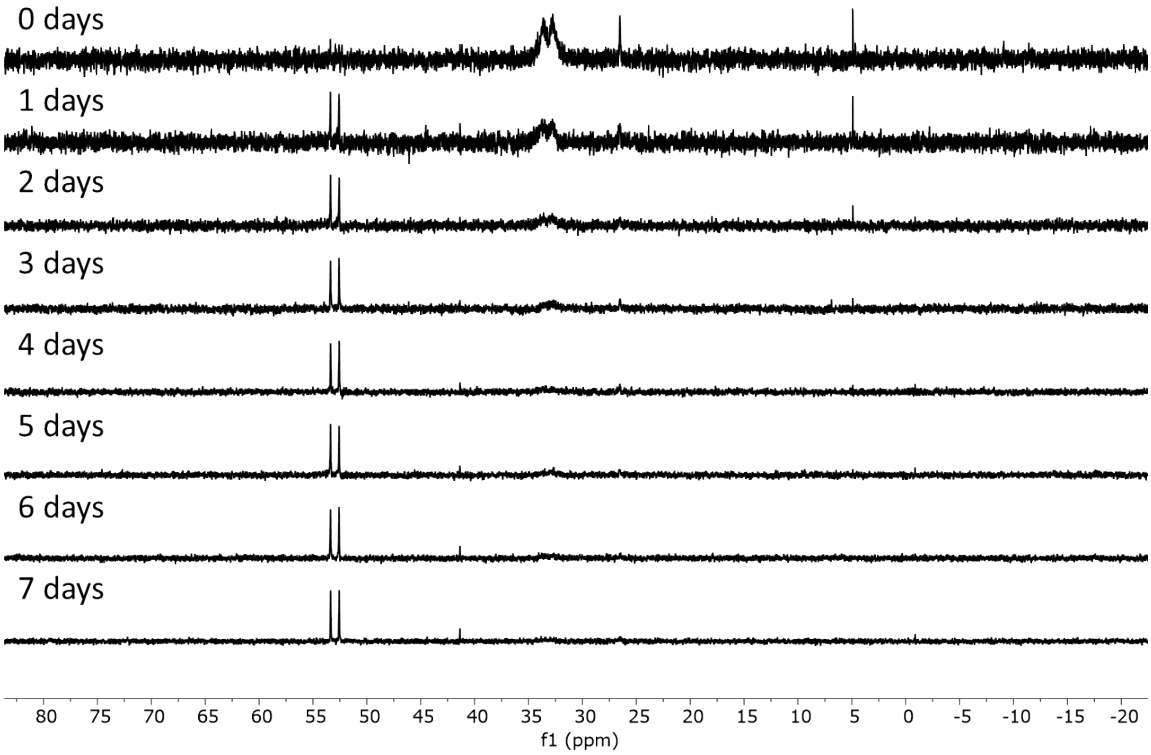

Figure S10. $^{31}P\{^1H\}$ NMR (162 MHz, CD_3CN, 298 K) spectra collected during the conversion of complex [**1**][OTf] into [**2**][OTf] over 1 week.

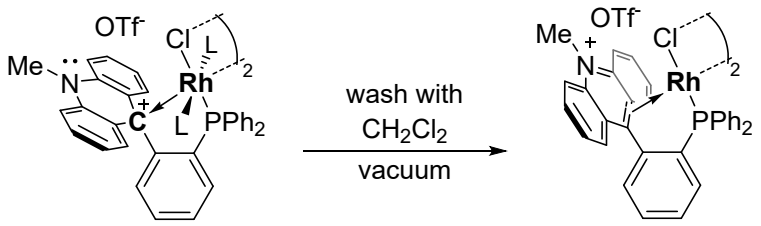

[**2**][OTf] [**3**][OTf]

Conversion of [**2**][OTf] into [**3**][OTf]: [**3**][OTf] (4 mg) in MeCN (0.6 mL) was loaded into a J. Young tube containing a sealed H_3PO_4/DMSO-d_6 capillary. The resulting red solution was subjected to $^{31}P\{^1H\}$ NMR spectroscopy, leading to a signal at 53.68 ppm (d, $^1J_{P-Rh}$ = 128.4 Hz) for [**2**][OTf]. The solvent from the J. Young tube was removed under a vacuum. The resulting residue was redissolved in CH_2Cl_2. This procedure was repeated three times. The residue was then dissolved in CH_2Cl_2 (0.6 mL), affording a dark green solution. The $^{31}P\{^1H\}$ NMR spectrum of this solution displayed a signal at 64.59 ppm (d, $^1J_{P-Rh}$ = 137.7 Hz) corresponding to [**3**][OTf].

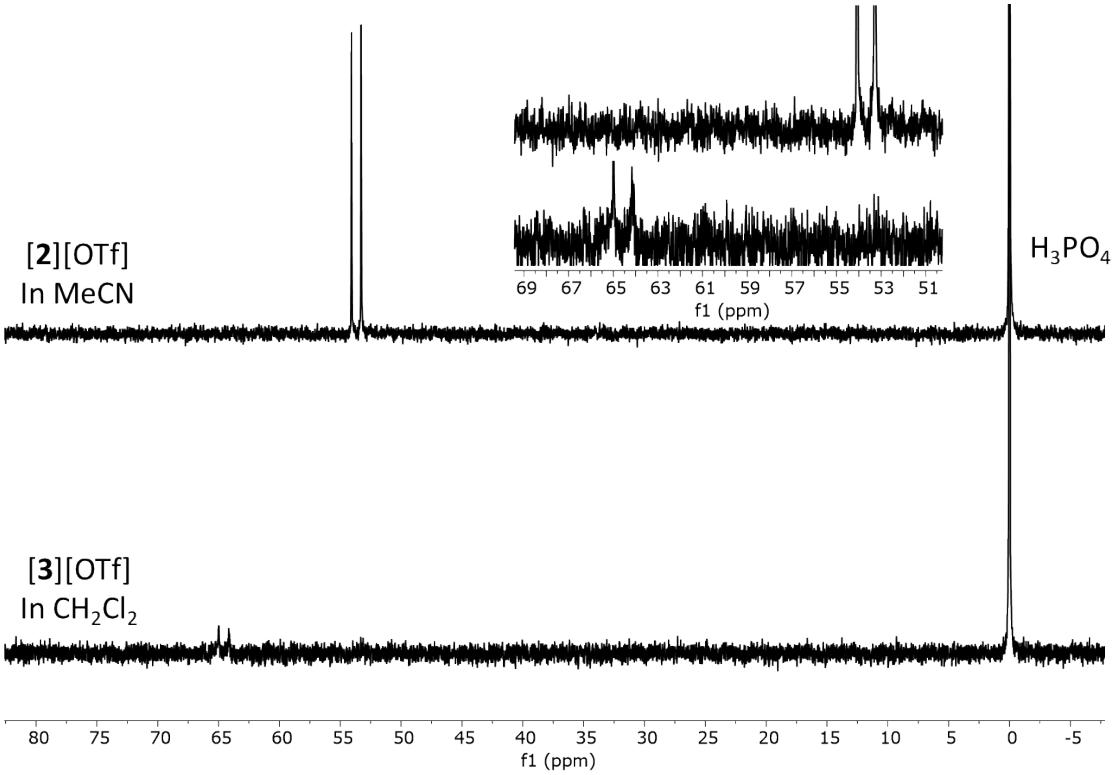

Figure S11. $^{31}P\{^1H\}$ NMR (162 MHz, DMSO-d_6, 298 K) spectra collected during the conversion of complex [**2**][OTf] into [**3**][OTf] (L = MeCN).

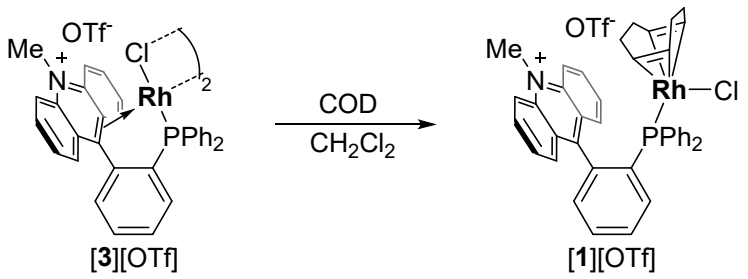

Conversion of [**3**][OTf] into [**1**][OTf] was done as follows: [**3**][OTf] (4 mg) was loaded into a J. Young tube containing a sealed H_3PO_4/DMSO-d_6 capillary and dissolved in CH_2Cl_2 (0.6 mL) forming a dark green solution. A ^{31}P NMR spectrum was collected. A signal at δ 64.64 (d, J = 137.3 Hz) was identified as [**3**][OTf] (referenced to the H_3PO_4/DMSO-d_6). Addition of cyclooctadiene (4 equiv., 1.2 μL) to the J. Young tube led to a change in color from green to yellow over a 10 minute period at which time a $^{31}P\{^1H\}$ NMR spectrum was collected. A signal at δ 33.88 (d, J = 150.8 Hz) was identified as [**1**][OTf] (referenced to the H_3PO_4/DMSO-d_6).

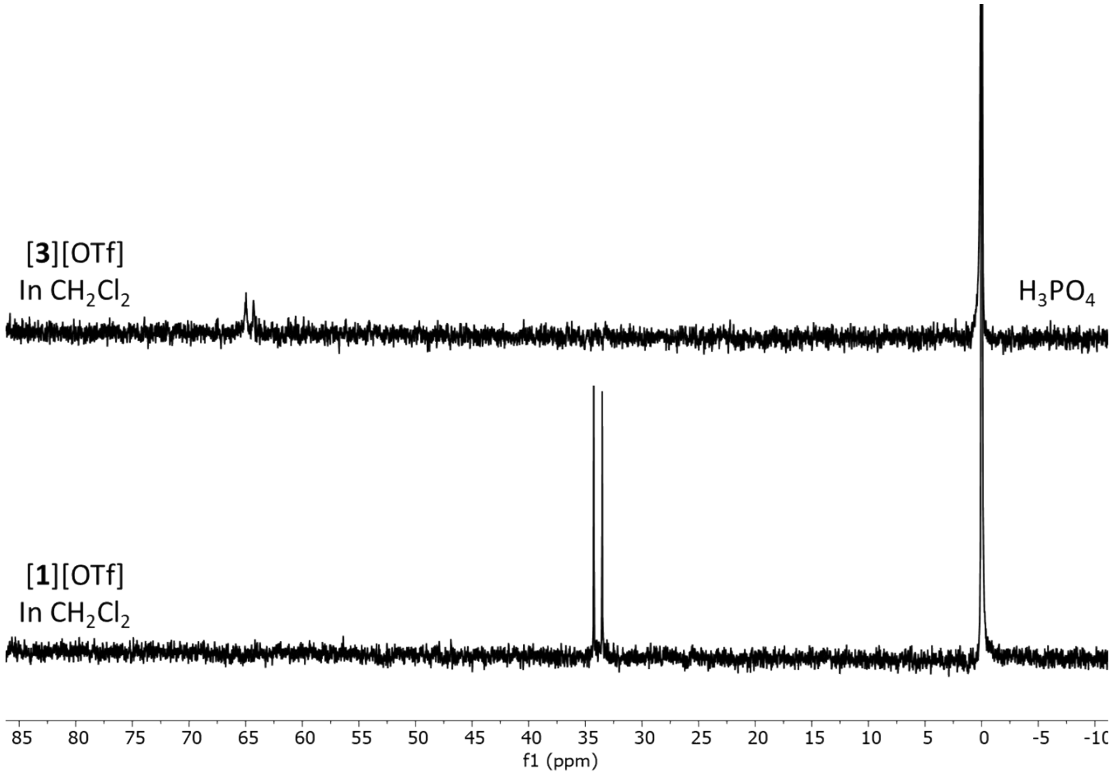

Figure S12. $^{31}P\{^1H\}$ NMR (202 MHz, DMSO-d_6, 298 K) spectrum of the conversion of complex [**3**][OTf] (top: 64.69 ppm) into [**1**][OTf] (Bottom: 33.88 ppm). Referenced internally to a capillary of 85% H_3PO_4 dissolved in DMSO-d_6.

Resitance of [**2**][OTf] to COD. [**3**][OTf] (4 mg) was loaded into a J. Young tube, dissolved CD_2Cl_2 (0.6 mL), and converted into [**2**][OTf] by addition of CD_3CN (0.1 mL), forming a dark green solution. Subsequently, an excess of cyclooctadiene (25 μL) was added to the J. Young tube, which left [**2**][OTf] unchanged as shown in Fig. S13.

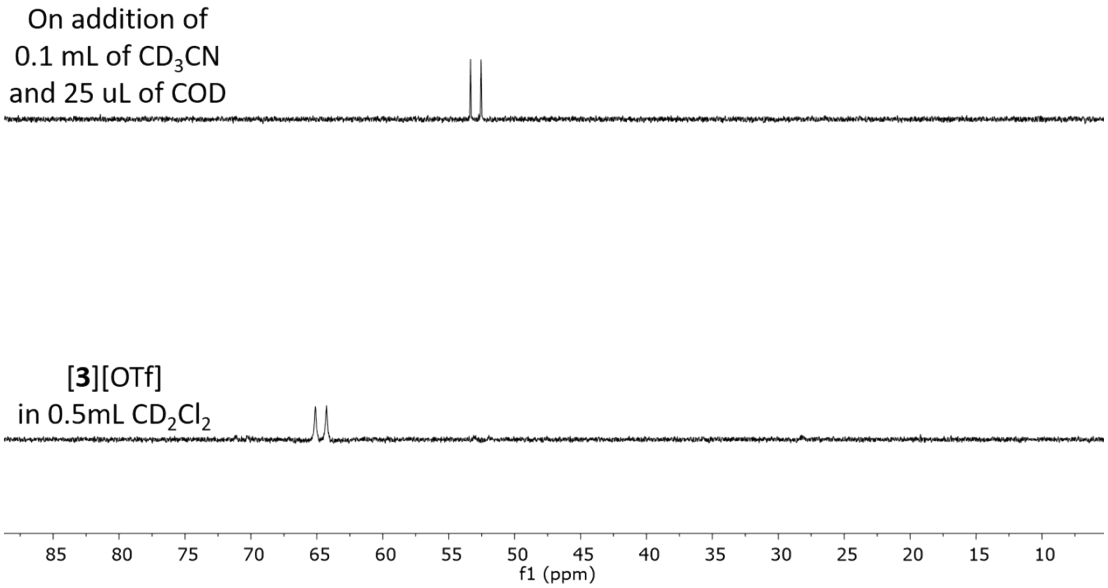

Figure S13. $^{31}P\{^1H\}$ NMR (202 MHz, 298 K) spectrum of the conversion of complex [**3**][OTf] into [**2**][OTf].

Stability of [**2**][OTf] in the presence of O_2. An NMR sample of [**2**][OTf] was generated by dissolving [**3**][OTf] (4 mg) in CH_2Cl_2 (0.6 ml) and MeCN (0.1 mL) inside a nitrogen-filled glove box. The headspace of the NMR tube was flushed with O_2 for 15 seconds. The sample was then sonicated for 1 minute and subjected to $^{31}P\{^1H\}$ NMR spectroscopy. The spectrum, displayed in Fig. S14, shows negligible decomposition of [**2**][OTf] even if the phosphine oxide [(*o*-$Ph_2P(O)(C_6H_4)Acr$)]$^+$ starts appearing at 26 ppm.

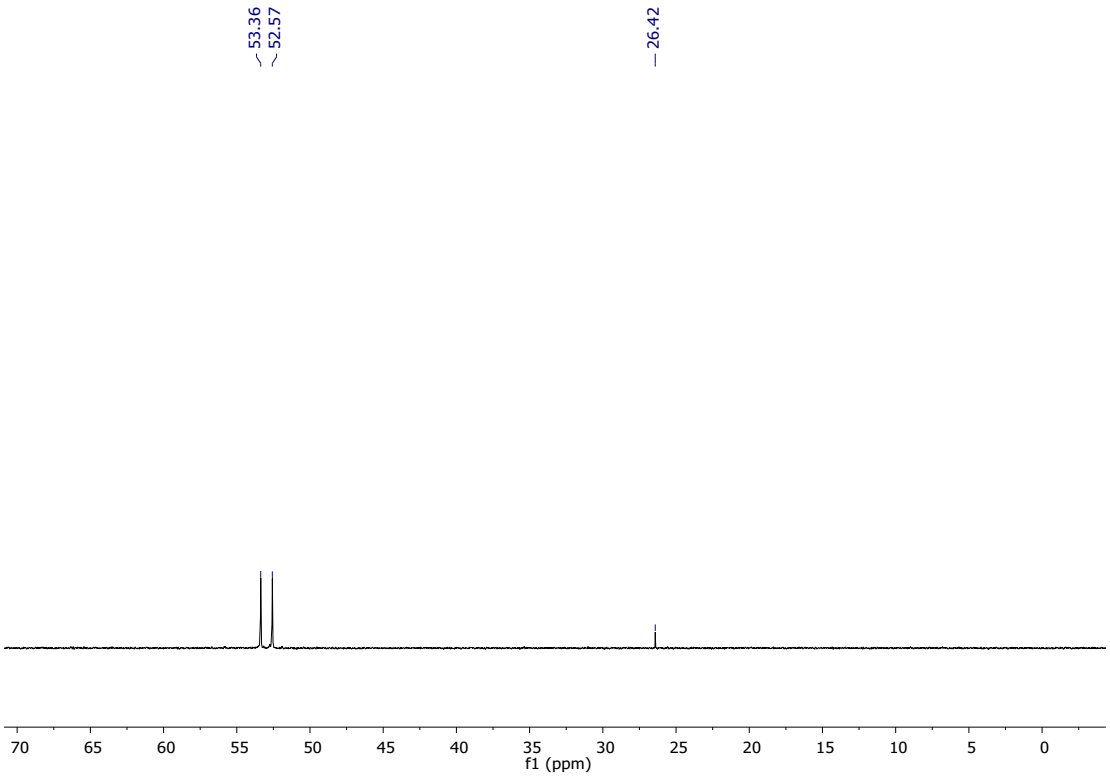

Figure S14. $^{31}P\{^1H\}$ NMR (202 MHz, 298 K) spectrum of a solution of [**2**][OTf] after exposure to O_2.

Stability of [**3**][OTf] in the presence of O_2. An NMR sample containing [**3**][OTf] (4 mg) in CH_2Cl_2 (0.6 ml) was prepared inside a nitrogen-filled glove box. The headspace of the NMR tube was flushed with O_2 for 15 seconds. The sample was then sonicated for 1 minute and subjected to $^{31}P\{^1H\}$ NMR spectroscopy. The spectrum, displayed in Fig. S15, shows almost complete decomposition of [**3**][OTf] and formation of the phosphine oxide $[(o\text{-}Ph_2P(O)(C_6H_4)Acr)]^+$ which appears at 27 ppm.

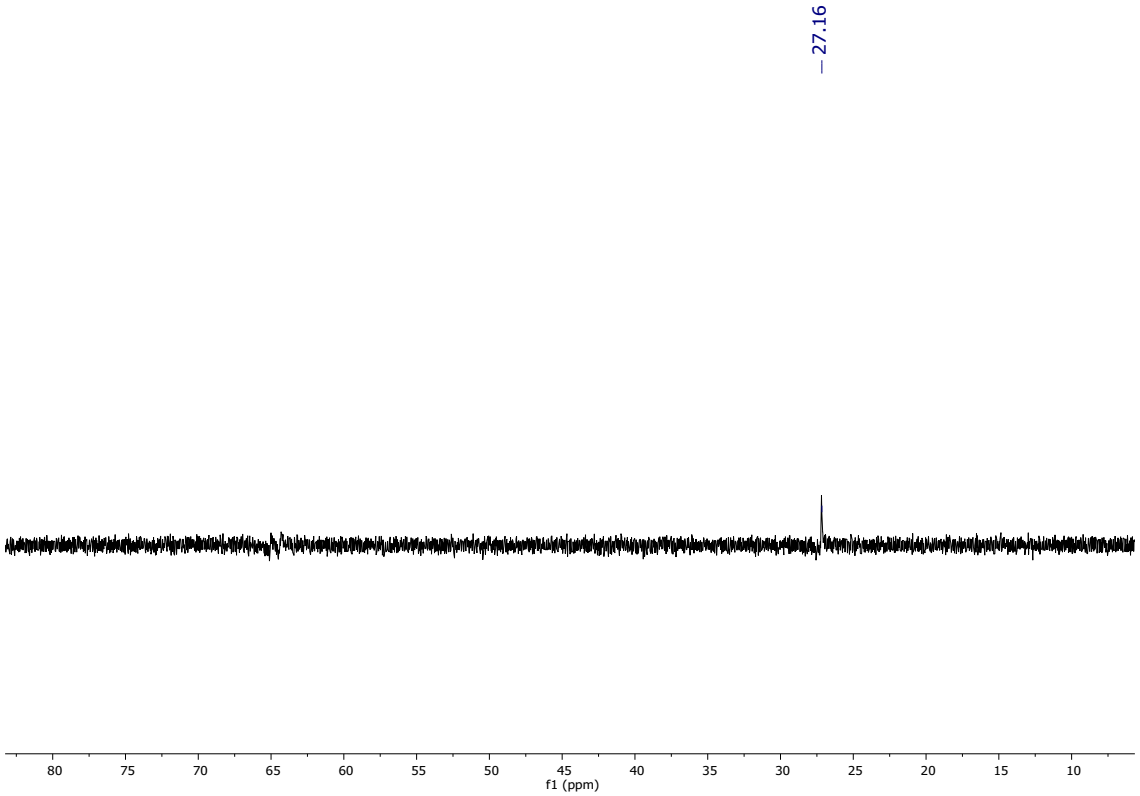

Figure S15. $^{31}P\{^1H\}$ NMR (202 MHz, 298 K) spectrum of a solution of [**3**][OTf] after exposure to O_2.

Stability of [**2**][OTf] in the presence of H_2O: An NMR sample of [**2**][OTf] was generated by dissolving [**3**][OTf] (4 mg) in CH_2Cl_2 (0.6 ml) and MeCN (0.1 mL) inside a nitrogen-filled glove box. This sample was combined with D_2O (15 μL), sonicated for 15 min and subjected to $^{31}P\{^1H\}$ NMR spectroscopy. The spectrum, displayed in Fig. S16, shows that [**2**][OTf] remains largely unperturbed by water.

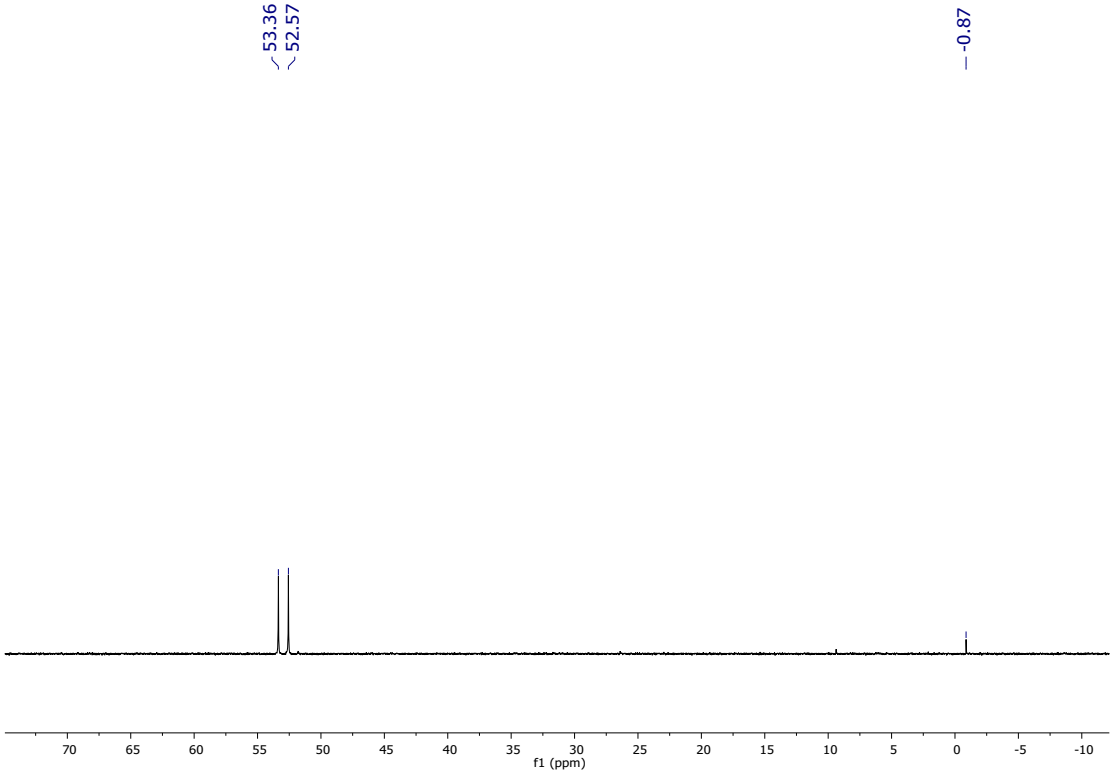

Figure S16. $^{31}P\{^1H\}$ NMR (202 MHz, 298 K) spectrum of a solution of [**2**][OTf] after addition of water.

Stability of [**3**][OTf] in the presence of H_2O: An NMR sample containing [**3**][OTf] (4 mg) in CH_2Cl_2 (0.6 ml) was prepared inside a nitrogen-filled glove box and combined with D_2O (15 μL). The tube was sonicated for 15 min and subjected to $^{31}P\{^1H\}$ NMR spectroscopy. The spectrum, displayed in Fig. S17, shows complete decomposition of [**3**][OTf].

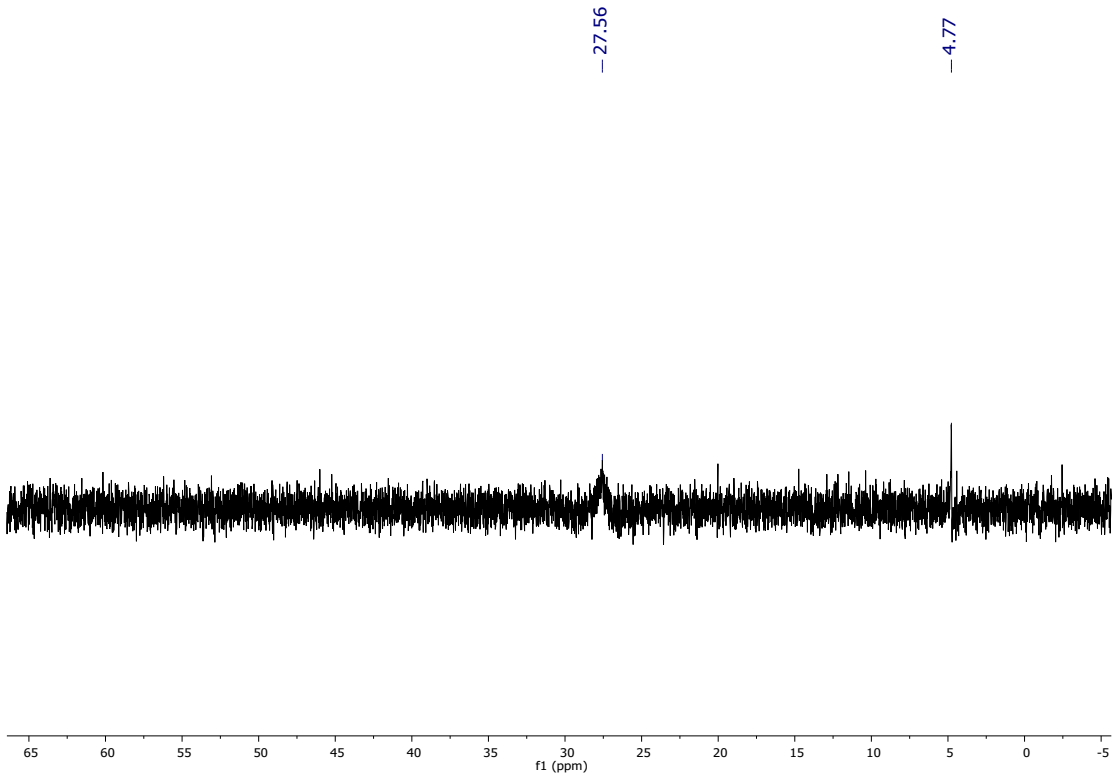

Figure S17. $^{31}P\{^1H\}$ NMR (202 MHz, 298 K) spectrum of a solution of [**3**][OTf] after addition of water.

3 Computational studies

3.1 General methods

The structures of [**2**][OTf] and [**3**][OTf] were optimized using DFT methods as implemented in Gaussian 16 using the MPW1PW91 functional and a mixed basis set defined as follows: cc-pVTZ-PP for Rh; 6-31G(d',p') for P/Cl; 6-31G(d') for C/N; and 6-31G for H. Frequency calculations, performed using the same level of theory on the optimized geometries, found no imaginary frequencies. NBO analysis was performed using BP86 as the functional and same basis set as mentioned above using the NBO 7.0 program. Pipek-Mezey calculations were carried out on the wave functions derived from the optimized structures using Multiwfn program.[2] The resulting NBO and Pipek-Mezey orbitals were visualized using the Avogadro program. [2]

3.2 Geometry optimized structures

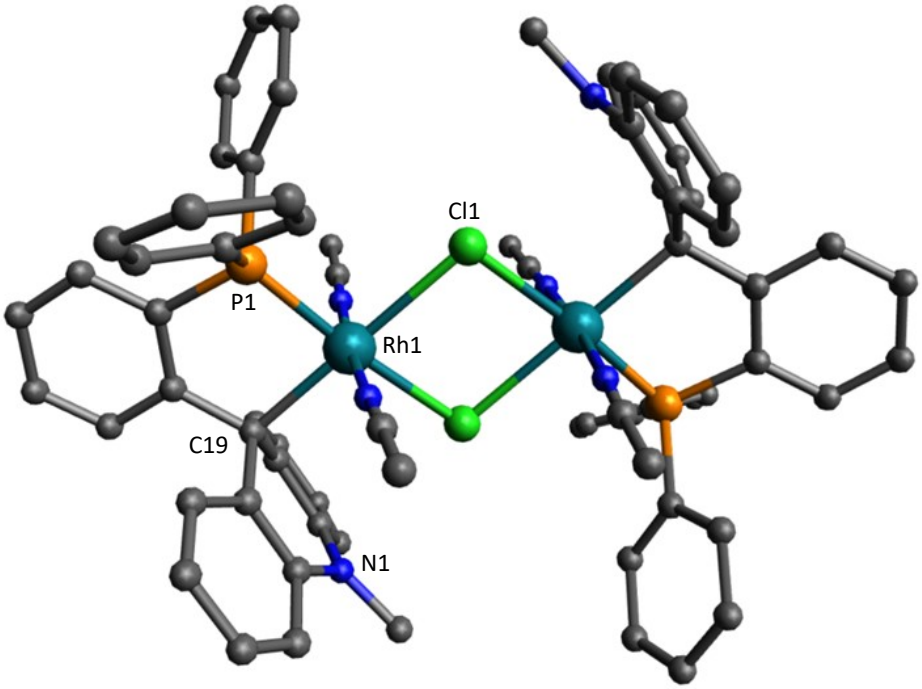

Figure S18. Optimized structure of [**2**][OTf] (hydrogen atoms omitted for clarity).

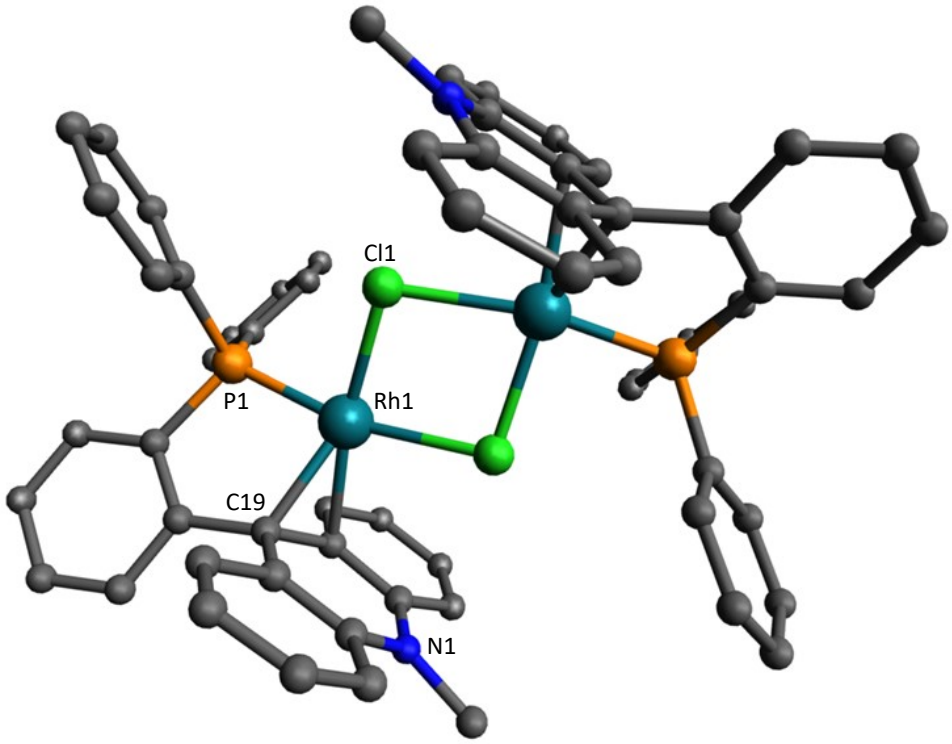

Figure S19. Optimized structure of [**3**][OTf] (hydrogen atoms omitted for clarity).

3.4 Pipek-Mezey LMOs

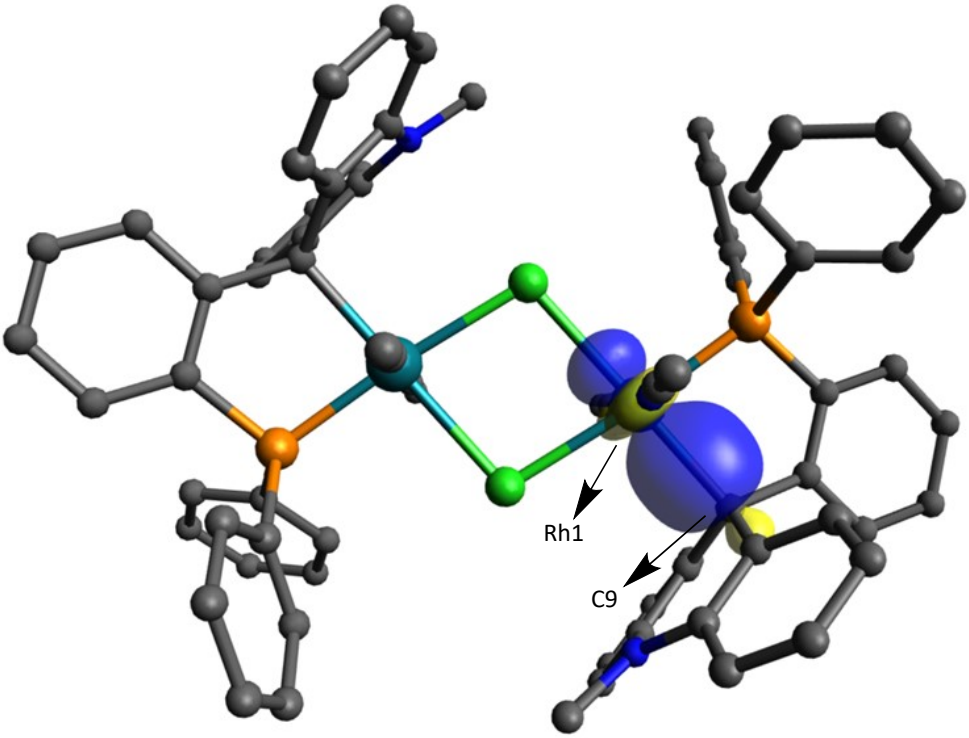

Figure S20. Pipek-Mezey orbital corresponding to the Rh1→C9 bonding in compound [**2**][OTf]. Parentage: Rh1: 47.1%; C9: 36.8%.

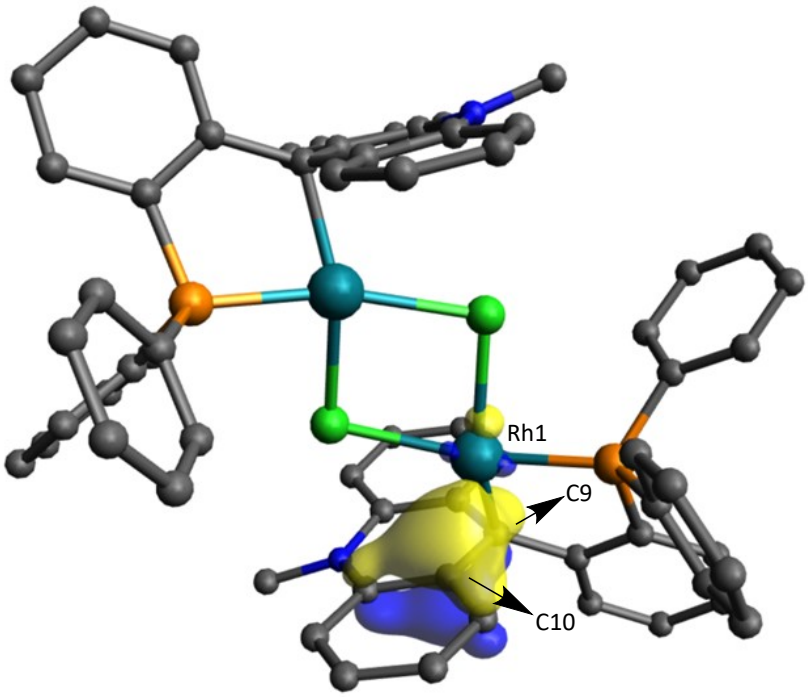

Figure S21. Pipek-Mezey orbital corresponding to the three-centers two-electron bond between C9-C10 and Rh1 in compound [**3**][OTf]. Parentage: Rh1: 17.0%; C10: 37.7%; C9: 12.3%.

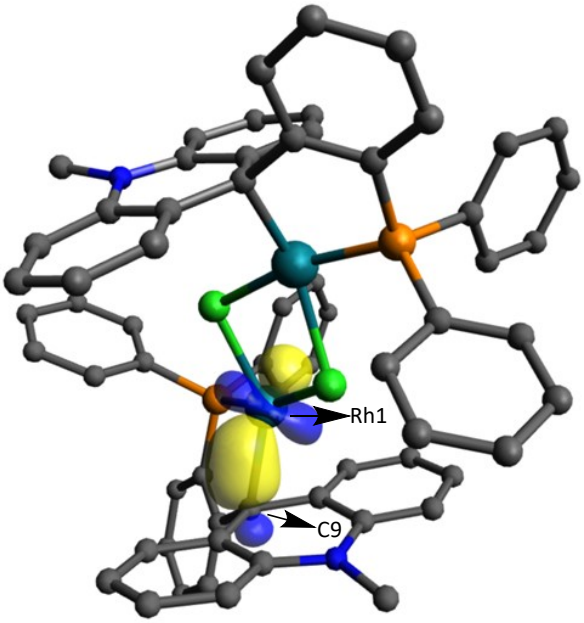

Figure S22. Pipek-Mezey orbital corresponding to the interaction between Rh1→C9 in compound [**3**][OTf]. Parentage: Rh1: 63.7%; C9: 20.5%.

3.5 NBO orbital analysis

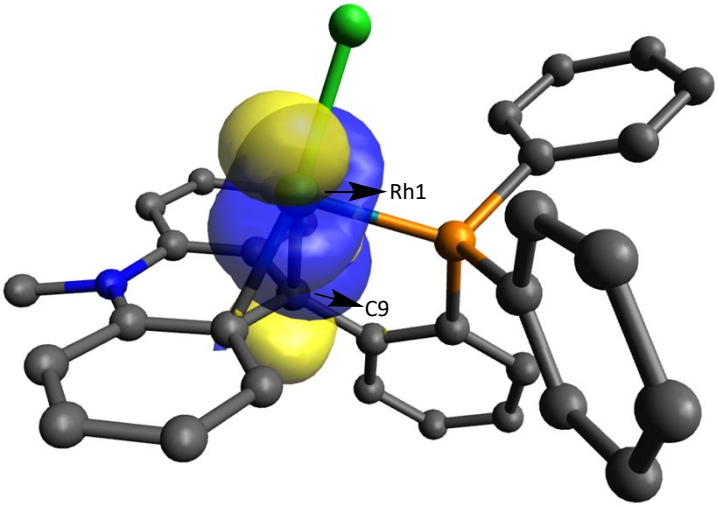

Figure S23. Truncated picture of NBO orbital corresponding to the z-type interaction between Rh1→C9 in compound [**3**][OTf].

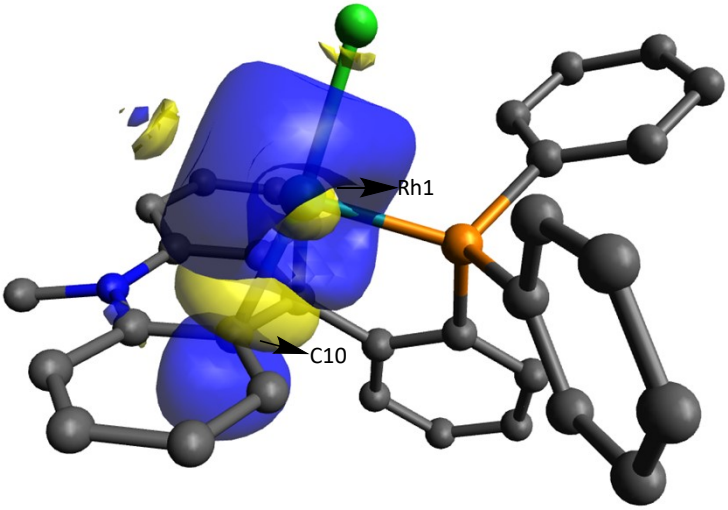

Figure S24. Truncated picture of NBO orbital corresponding to the L-type interaction between C10→Rh1 in compound [**3**][OTf].

3.6 Cartesian coordinates of geometry optimized structures

Table S1. Cartesian coordinates for [**2**][OTf].

Atom Number	Coordinates X	Y	Z
Rh1	-1.95468	0.14881	-0.13534
Rh2	1.95471	-0.14879	0.13531
Cl3	0.05576	1.62139	-0.22375
Cl4	-0.05576	-1.62133	0.22366
P5	-3.65979	-1.33917	-0.08503
P6	3.65986	1.33915	0.08508
N7	-1.79882	-0.17406	-2.07169
N8	-1.98524	0.39162	1.82423
N9	-2.11447	4.04664	0.16507
N10	1.79882	0.17403	2.07167
N11	1.98532	-0.39156	-1.82427
N12	2.11426	-4.04654	-0.16517
C13	-3.76912	2.39748	0.81283
C14	-3.54903	1.65252	-0.47045
C15	-3.11717	-2.52479	2.38369
C16	-3.03542	2.57769	-1.53106
C17	-5.91015	1.74127	-1.37144
C18	-1.97924	0.49427	2.97102
C19	-3.00344	3.54989	1.10689
C20	-4.1151	-1.97056	1.56755
C21	-4.84422	0.96056	-0.89491
C22	-1.6842	-0.39336	-3.19643
C23	-3.26049	2.33842	-2.8963
C24	-4.70683	1.96652	1.7634
C25	-2.29852	3.73146	-1.17317
C26	-7.12371	1.16152	-1.72096
C27	-4.87501	2.61061	2.9824
C28	-5.05476	-0.41451	-0.75992
C29	-4.09545	3.73203	3.27149
C30	-3.17594	4.20115	2.343
C31	-3.48158	-2.82617	-1.13928
C32	-2.00697	0.6111	4.41279
C33	-1.59026	-0.6548	-4.61578
C34	-2.75245	3.16547	-3.88897
C35	-6.27689	-1.0069	-1.11752
C36	-5.43382	-1.91638	2.03476
C37	-3.44103	-3.03438	3.63861
C38	-7.31179	-0.2186	-1.60098
C39	-5.75	-2.42112	3.29575
C40	-3.00133	-4.03528	-0.6195
C41	-2.85278	-5.14651	-1.44748
C42	-2.00359	4.28565	-3.52196
C43	-3.81213	-2.75163	-2.50089
C44	-1.15174	5.06093	0.54445
C45	-4.75784	-2.98309	4.09687
C46	-1.78752	4.57121	-2.18109
C47	-3.1803	-5.06472	-2.8
C48	-3.66255	-3.86565	-3.32358
C49	3.76902	-2.39748	-0.8129
C50	3.54899	-1.65255	0.4704
C51	3.1173	2.52483	-2.38364
C52	3.03534	-2.57771	1.53099
C53	5.91011	-1.7414	1.37141
C54	1.97944	-0.49416	-2.97106
C55	3.00326	-3.54983	-1.10698
C56	4.11521	1.97059	-1.56747
C57	4.8442	-0.96064	0.89489
C58	1.68417	0.39328	3.19641
C59	3.26043	-2.33849	2.89624
C60	4.70671	-1.96653	-1.76349
C61	2.29836	-3.73142	1.17308
C62	7.12368	-1.16169	1.72097
C63	4.87481	-2.61058	-2.98253
C64	5.05479	0.41442	0.75994
C65	4.09518	-3.73194	-3.27162
C66	3.17567	-4.20104	-2.34312
C67	3.48165	2.82609	1.13941
C68	2.00731	-0.61057	-4.41286
C69	1.59037	0.65459	4.6158
C70	2.75235	-3.16553	3.8889
C71	6.27694	1.00676	1.11757
C72	5.43394	1.91642	-2.03465
C73	3.44119	3.03444	-3.63854
C74	7.3118	0.21843	1.60102
C75	5.75015	2.42119	-3.29562
C76	3.00142	4.03525	0.6197
C77	2.85287	5.14642	1.44776
C78	2.00341	-4.28565	3.52186
C79	3.81218	2.75146	2.50102
C80	1.15146	-5.06076	-0.54457
C81	4.75802	2.98317	-4.09676
C82	1.78731	-4.57116	2.18099
C83	3.18038	5.06454	2.80028
C84	3.66261	3.86543	3.32378
H85	-2.08491	-2.55079	2.04343
H86	-5.78146	2.81547	-1.47202
H87	-3.84739	1.47142	-3.18337
H88	-5.30567	1.08689	1.54779
H89	-7.92953	1.78903	-2.09311
H90	-5.60698	2.24356	3.69662
H91	-4.21728	4.26088	4.21339
H92	-2.61762	5.10346	2.56588
H93	-3.04109	0.52417	4.76017
H94	-1.60566	1.58309	4.7139
H95	-1.40698	-0.18746	4.85874
H96	-2.59848	-0.68057	-5.04176
H97	-1.10135	-1.61883	-4.78438
H98	-1.01426	0.1391	-5.1
H99	-2.94567	2.94484	-4.93524
H100	-6.40828	-2.08148	-1.02032
H101	-6.21887	-1.48141	1.42414
H102	-2.66105	-3.46629	4.26019
H103	-8.25821	-0.67228	-1.88161
H104	-6.77672	-2.37337	3.64858
H105	-2.75056	-4.12476	0.43244
H106	-2.48659	-6.07992	-1.02854
H107	-1.6075	4.95718	-4.27961
H108	-4.20335	-1.83032	-2.92189
H109	-1.56759	6.07712	0.50647
H110	-0.28864	5.00516	-0.12075
H111	-0.79601	4.86092	1.55722
H112	-5.0085	-3.37742	5.0781
H113	-1.24899	5.47415	-1.91597
H114	-3.06896	-5.93457	-3.44187
H115	-3.93177	-3.79529	-4.37415
H116	2.08502	2.55079	-2.04342
H117	5.78138	-2.8156	1.47197
H118	3.8474	-1.47153	3.18332
H119	5.30561	-1.08694	-1.54787
H120	7.92947	-1.78925	2.09311
H121	5.60678	-2.24354	-3.69676
H122	4.21695	-4.26076	-4.21355
H123	2.61729	-5.10331	-2.56602
H124	3.04142	-0.52316	-4.76014
H125	1.60638	-1.58263	-4.71426
H126	1.40705	0.18789	-4.85864
H127	2.59862	0.68013	5.04172
H128	1.10164	1.61868	4.78453
H129	1.01426	-0.13927	5.09997
H130	2.94559	-2.94494	4.93517
H131	6.40836	2.08134	1.0204
H132	6.21897	1.48145	-1.42401
H133	2.66122	3.46634	-4.26014
H134	8.25824	0.67206	1.88167
H135	6.77689	2.37345	-3.64841
H136	2.75067	4.1248	-0.43222
H137	2.4867	6.07986	1.02888
H138	1.60728	-4.95718	4.2795
H139	4.20339	1.83012	2.92197
H140	1.56724	-6.07697	-0.50663
H141	0.28837	-5.00494	0.12064
H142	0.79573	-4.86068	-1.55733
H143	5.00871	3.37752	-5.07798
H144	1.24872	-5.47405	1.91585
H145	3.06904	5.93435	3.4422
H146	3.93182	3.795	4.37435

Table S2. Cartesian coordinates for [**3**][OTf].

Atom Number	Coordinates X	Y	Z
Rh1	1.73093	-0.5562	0.12461
Rh2	-1.73092	0.55619	0.12463
Cl3	0.54828	1.45949	-0.15879
Cl4	-0.54827	-1.45949	-0.15883
P5	3.5492	0.66826	0.62227
P6	-3.54921	-0.66828	0.62226
N7	1.24694	-3.91514	-1.31061
N8	-1.2469	3.91515	-1.3105
C9	4.96241	-0.27297	-0.00543
C10	2.65897	-2.11901	-2.15151
C11	1.55654	-3.62121	-0.01427
C12	6.30517	0.11399	0.07893
C13	1.67029	-3.11066	-2.36551
C14	3.71718	2.3169	-0.14113
C15	0.9795	-4.31041	1.06472
C16	3.15348	-1.8457	-0.80995
C17	4.59579	-1.43814	-0.6839
C18	2.52493	-2.58333	0.27099
C19	3.74226	0.92235	2.4158
C20	2.69317	1.55705	3.0996
C21	3.68305	3.66496	-2.15075
C22	5.59375	-2.24095	-1.24973
C23	4.18501	3.41776	0.58466
C24	3.46102	2.44888	-1.51326
C25	0.44086	-5.09817	-1.60115
C26	3.15001	-1.39518	-3.25707
C27	2.91403	-2.36914	1.63088
C28	3.8918	1.30451	5.18136
C29	1.33802	-4.01218	2.3712
C30	1.62795	-2.53376	-4.7194
C31	4.39952	4.63615	-0.05882
C32	2.30626	-3.04837	2.6702
C33	2.77422	1.75033	4.47469
C34	4.15347	4.76049	-1.42399
C35	2.64772	-1.59277	-4.52677
C36	4.85973	0.47322	3.12975
C37	6.93056	-1.87237	-1.13837
C38	1.14815	-3.28456	-3.6611
C39	7.28862	-0.69205	-0.48297
C40	4.93056	0.66557	4.50896
C41	-4.96242	0.273	-0.00537
C42	-2.65899	2.11908	-2.15143
C43	-1.5565	3.62119	-0.01416
C44	-6.30517	-0.11395	0.079
C45	-1.67029	3.11072	-2.36541
C46	-3.71723	-2.31688	-0.1412
C47	-0.97941	4.31032	1.06486
C48	-3.15348	1.84573	-0.80988
C49	-4.59579	1.43819	-0.68381
C50	-2.5249	2.58333	0.27108
C51	-3.74224	-0.92244	2.41579
C52	-2.69315	-1.55717	3.09955
C53	-3.6832	-3.66485	-2.15088
C54	-5.59375	2.24104	-1.24959
C55	-4.18504	-3.41777	0.58455
C56	-3.46113	-2.44879	-1.51335
C57	-0.4408	5.09815	-1.60108
C58	-3.15005	1.39529	-3.25701
C59	-2.91399	2.3691	1.63096
C60	-3.89174	-1.30471	5.18134
C61	-1.33792	4.01205	2.37133

Atom Number	Coordinates X	Y	Z
C62	-1.62801	2.53395	-4.71933
C63	-4.39958	-4.63613	-0.05897
C64	-2.30619	3.04826	2.67031
C65	-2.77417	-1.75051	4.47464
C66	-4.15359	-4.7604	-1.42416
C67	-2.64778	1.59295	-4.52672
C68	-4.85971	-0.47333	3.12977
C69	-6.93056	1.87246	-1.13822
H70	-1.14819	3.28469	-3.661
H71	-7.28863	0.69212	-0.48285
H72	-4.93051	-0.66575	4.50897
H73	6.5764	1.04753	0.56494
H74	0.21665	-5.05917	0.89628
H75	1.81628	1.89736	2.55374
H76	3.49739	3.75714	-3.21749
H77	5.32328	-3.14951	-1.78094
H78	4.38978	3.32805	1.64733
H79	3.0841	1.6007	-2.07963
H80	0.65807	-5.8741	-0.86769
H81	0.72552	-5.49552	-2.57462
H82	-0.62995	-4.86704	-1.59114
H83	3.93641	-0.66564	-3.08877
H84	3.76174	-1.72943	1.83995
H85	3.9522	1.45581	6.25525
H86	0.86001	-4.56195	3.17755
H87	1.20775	-2.68648	-5.70904
H88	4.77111	5.48467	0.50854
H89	2.60322	-2.85582	3.69542
H90	1.96192	2.24628	4.99863
H91	4.33581	5.70731	-1.92463
H92	3.03558	-1.02326	-5.36538
H93	5.67835	-0.02517	2.61851
H94	7.69868	-2.5019	-1.57804
H95	0.34814	-3.99053	-3.84537
H96	8.33228	-0.39885	-0.42029
H97	5.80302	0.31882	5.05518
H98	-6.57641	-1.04751	0.56497
H99	-0.21652	5.05905	0.89646
H100	-1.81626	-1.89745	2.55366
H101	-3.49759	-3.75698	-3.21764
H102	-5.32328	3.14961	-1.78078
H103	-4.38976	-3.32811	1.64724
H104	-3.08423	-1.60059	-2.0797
H105	-0.65803	5.87414	-0.8677
H106	-0.72543	5.49544	-2.5746
H107	0.63	4.86701	-1.59103
H108	-3.93645	0.66575	-3.08873
H109	-3.76171	1.72939	1.84002
H110	-3.95213	-1.45606	6.25522
H111	-0.85987	4.56176	3.1777
H112	-1.20784	2.68672	-5.70897
H113	-4.77116	-5.48467	0.50837
H114	-2.60314	2.85568	3.69552
H115	-1.96187	-2.24648	4.99854
H116	-4.33597	-5.7072	-1.92483
H117	-3.03567	1.02348	-5.36534
H118	-5.67833	0.02508	2.61856
H119	-7.69868	2.50202	-1.57785
H120	-0.34819	3.99069	-3.84525
H121	-8.33228	0.39893	-0.42017
H122	-5.80297	-0.31902	5.05522

4 X-ray diffraction analysis

4.1 Experimental details

The crystallographic measurements were performed at 110(2) K using a three circle (Quest; Mo Kα radiation, λ = 0.71073 Å) and kappa (Venture; Cu Kα radiation, λ = 1.54178 Å) Bruker-AXS with IμS source and a Photon III area detector diffractometer. In each case, a specimen of suitable size and quality was selected and mounted onto a nylon loop and cooled to 110(2) K in a cold nitrogen stream (OXFORD Crysosystems). The data was collected and reduced using Bruker AXS APEX 3 software[3] and solved by direct methods. Semiempirical absorption corrections were applied using SADABS.[4] Subsequent refinement using a difference map on F^2 using the SHELXTL/PC package (version 6.1 & OLEX^2).[5] Thermal parameters were refined anisotropically for all non-hydrogen atoms to convergence. H atoms were added at idealized positions using a riding model. The results of these X-ray measurements are provided as CIF files. CCDC 2421484-2421486 contain the supplementary crystallographic data for this paper.

4.2 Table showing the compounds characterized by X-ray diffraction and their corresponding CCDC numbers.

Compound	CCDC
[**1**][OTf]	2421484
[**2**][OTf]	2421485
[**3**][OTf]	2421486

4.2 Solid state structures

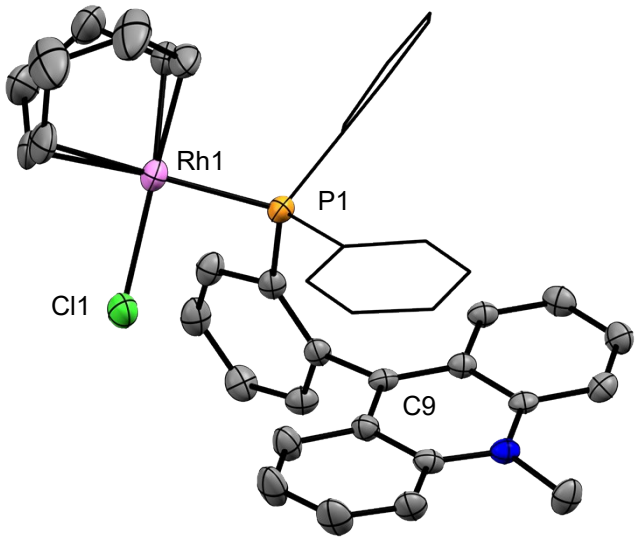

Figure S25. Solid-state structure of [**1**][OTf]. Crystallized by layering diethyl ether over a solution of [**1**][OTf] in dichloroethane. Hydrogen atoms and solvent molecules were omitted for clarity. Selelected bond length and angles: Rh1-P1 = 2.3191(12) Å, Rh1-Cl1 = 2.3752(14) Å, Rh1-C9 = 5.381(4) Å, Cl1-Rh1-P1 = 89.74(5)°.

5 References

1. L. C. Wilkins, Y. Kim, E. D. Litle and F. P. Gabbaï, *Angew. Chem. Int. Ed.*, 2019, **58**, 18266-18270.
2. a) M. D. Hanwell, D. E. Curtis, D. C. Lonie, T. Vandermeersch, E. Zurek and G. R. Hutchison, *Journal of Cheminformatics*, 2012, **4**, 17; b) J. Pipek and P. G. Mezey, *J. Chem. Phys.*, 1989, **90**, 4916-4926.
3. Bruker, 2019, APEX3 (v2019.2011-2010), Bruker AXS Inc., Madison, Wisconsin, USA.
4. G. M. Sheldrick, *Journal*, 2016.
5. a) G. M. Sheldrick, *Acta Crystallographica Section A*, 2015, **71**, 3-8; b) O. V. Dolomanov, L. J. Bourhis, R. J. Gildea, J. A. K. Howard and H. Puschmann, *J. Appl. Crystallogr.*, 2009, **42**, 339-341.